Post-interventional atherosclerotic vascular remodeling : preclinical investigation into immune-modulatory therapies

Ewing, M.M.

Chapter 7

Blocking Toll-Like Receptors 7 and 9 Reduces Postinterventional Remodeling via Reduced Macrophage Activation, Foam Cell Formation, and Migration

J.C Karper[1, 2], M.M. Ewing[1, 2, 3], K.L.L. Habets[4], M.R de Vries[1, 2], H.A.B Peters[1,2], A.M. van Oeveren-Rietdijk[2,5], H.C. de Boer[2,5], J.F Hamming[1], J. Kuiper[4], E.R. Kandimalla[6], N. La Monica[6], J.W. Jukema[2, 3], P.H.A. Quax[1, 2]

1 Dept. of Surgery, Leiden University Medical Center (LUMC), Leiden, The Netherlands
2 Einthoven Laboratory for Experimental Vascular Medicine, LUMC, Leiden, The Netherlands
3 Department of Cardiology, LUMC, Leiden, The Netherlands
4 Department of Biopharmaceutics, Leiden University, Leiden, The Netherlands
5 Department of Nephrology, LUMC, Leiden, The Netherlands
6 Idera Pharmaceuticals, Boston, Massachusetts, USA

Arterioscler Thromb Vasc Biol. 2012;32:e72-80

Abstract

Objective The role of toll-like receptors (TLRs) in vascular remodeling is well established. However, the involvement of the endosomal TLRs is unknown. Here, we study the effect of combined blocking of TLR7 and TLR9 on postinterventional remodeling and accelerated atherosclerosis.

Methods and Results In hypercholesterolemic apolipoprotein E*3-Leiden mice, femoral artery cuff placement led to strong increase of TLR7 and TLR9 presence demonstrated by immunohistochemistry. Blocking TLR7/9 with a dual antagonist in vivo reduced neointimal thickening and foam cell accumulation 14 days after surgery by 65.6% (P=0.0079). Intima/media ratio was reduced by 64.5% and luminal stenosis by 62.8%. The TLR7/9 antagonist reduced the arterial wall inflammation, with reduced macrophage infiltration, decreased cytoplasmic high-mobility group box 1 expression, and altered serum interleukin-10 levels. Stimulation of cultured macrophages with TLR7 and TLR9 ligands enhanced tumor necrosis factor-α expression, which is decreased by TLR7/9 antagonist coadministration. Additionally, the antagonist abolished the TLR7/9-enhanced low-density lipoprotein uptake. The antagonist also reduced oxidized low-density lipoprotein–induced foam cell formation, most likely not via decreased influx but via increased efflux, because CD36 expression was unchanged whereas interleukin-10 levels were higher (36.1±22.3 pg/mL versus 128.9±6.6 pg/mL; P=0.008).

Conclusion Blocking TLR7 and TLR9 reduced postinterventional vascular remodeling and foam cell accumulation indicating TLR7 and TLR9 as novel therapeutic targets.

Introduction

Postinterventional remodeling is a critical determinant of long-term efficacy of percutaneous coronary interventions. Restenosis is characterized by acute elastic recoil and intimal hyperplasia attributable to inflammation, smooth muscle cell (SMC) proliferation, and extracellular matrix turnover.[1] Under hypercholesterolemic conditions, this is accompanied by influx and accumulation of low-density lipoprotein (LDL) cholesterol in the vessel wall that becomes oxidized and taken up by macrophages. Thereby these macrophages become foam cells and initiate a process of accelerated atherosclerosis.[2] Previously, we and others described an important causal role for extracellular toll-like receptors (TLRs) in postinterventional remodeling. It has been shown that TLR4 and the MyD88-dependent pathway play an important role in restenosis and postinterventional accelerated atherosclerosis.[3–6] Similarly, a crucial role for TLR2 has been described.[7]

TLRs, as part of the innate immune system, are pattern recognition receptors known to recognize exogenous ligands that originate from bacteria or viruses as well as endogenous ligands. These endogenous ligands may be released after tissue damage or cell stress, processes that may be initiated by percutaneous coronary interventions. MyD88-dependent signaling is the dominant activation pathway of TLR signaling leading to nuclear factor-kappaB activation and upregulation of several proinflammatory cytokines. Because TLR2 and TLR4 are known to be expressed on the cell surface of vascular cells and activated in vascular disease processes via damage-associated molecular patterns as endogenous ligands, such as heat shock proteins, fibronectin containing extradomain A, tenascin-C, and high-mobility group box 1 (HMGB1),[8–11] research in the cardiovascular field mainly focused on TLR2 and TLR4. Little is known about the role of endosomal TLRs that are mostly studied for their recognition of viral/bacterial DNA and RNA fragments, and were originally considered absent in the healthy arterial vessel wall.[12] Activation of endosomal TLRs like TLR7 and TLR9 may lead to upregulation of interferon-α (IFN-α), interleukin-6 (IL-6), IL-12, or tumor necrosis factor-α (TNF-α) by innate immune cells (eg, macrophages). Recently, increased TLR7 mRNA was found in atheroma of human carotids.[13] Moreover, TLR9 was also found in human atherosclerotic plaques,[14] and arterial cells were responsive to TLR9 ligand.[15] Interestingly, it has been suggested that these receptors may also recognize self-DNA/RNA that is exposed after cell stress and damage causing a sterile inflammatory reaction.[16–19] TLR7 and TLR9 have also been shown to recognize immune complexes containing selfnucleic
acids in autoimmune diseases.[16,20] Percutaneous coronary interventions are considered to cause severe damage to the endothelium allowing influx of lipids and inflammatory cells into the vessel wall. Concurrently, deeper layers in the vessel wall experience severe stress, and cellular death at the place of intervention may cause a release of self-RNA/DNA or proteins that enhance the direct recognition of nucleic acids by intracellular TLRs or binding of these nucleic acids to intracellular TLR signaling regulators such as HMGB1.[21] Most interestingly, activation of TLR9 is also reported to increase the secretion of HMGB1, the endogenous ligand for TLR4.[22]

Recently, we have identified a novel class of oligonucleotidebased compounds that act as dual antagonists of TLR7 and TLR9, and inhibit immune responses mediated through these receptors.[23,24] In the present study, we focus on the therapeutic poten-

tial of targeting TLR7 and TLR9 to reduce postinterventional remodeling by preventing neointima formation and accelerated atherosclerosis. We illustrate the presence and upregulation of TLR7 and TLR9 and their colocalization with macrophages/foam cells in a murine model for neointima formation and accelerated atherosclerosis. A causal role of the TLR7/9 was studied in a murine model for postinterventional vascular remodeling in hypercholesterolemic apolipoprotein E*3-Leiden (apoE*3-Leiden) mice by the use of the TLR7/9 antagonist. Furthermore, we studied activation and antagonism of TLR7 and TLR9 on cultured macrophages and on foam cell formation using a novel TLR7/9 dual antagonist.

Materials and Methods

A detailed description of all materials and methods used is available in the online-only Data Supplement. In brief, nonconstricted polyethylene cuffs were placed around the femoral arteries as a well-established model for neointima formation and accelerated atherosclerosis in hypercholesterolemic apoE3-Leiden mice. Immunohistochemistry for TLR7 and TLR9 was performed on paraffin-embedded sections of cuffed arteries of hypercholesterolemic apoE3-Leiden mice at t=0 and t=14. A TLR7/TLR9 dual antagonist was synthesized, and specificity was determined. We studied its effect on neointima formation and accelerated atherosclerosis in hypercholesterolemic apoE*3-Leiden mice after femoral arterial cuff placement by injecting the antagonist biweekly to get sufficient TLR7/9 blockade. Intimal lesions were analyzed for CD45, MAC3, and HMGB1 by immunohistochemistry. The antagonist was used to study the effect of blocking of TLR7/9 on macrophage activation and lipid accumulation in macrophages. Cytokine levels of TNF-α, IFN-γ–induced protein 10, IL-6, IL-12, and IL-10 were quantified by ELISA.

Results

Arterial Injury Leads to TLR7 and TLR9 Presence in the Vessel Wall

Little is known about the presence of TLR7 and TLR9 in the vessel wall after surgical intervention. Using immunohistochemical analysis, we explored whether TLR7 and TLR9 are expressed in cuffed remodeled arteries with neointimal lesions after 14 days and in noncuffed arteries of hypercholesterolemic apoE*3-Leiden mice, because TLR expression may differ among different arterial segments and also in response to vessel damage.[12,13] Cuff placement for 14 days provoked severe neointimal thickening, and showed the presence of TLR7/9 profoundly in the tunica media of these arterial segments. Presence of either TLR7 or TLR9 could not be observed in noncuffed femoral arteries (Figure 1A–1D). Lesions in cuffed arteries of wild-type mice on a chow diet that consist dominantly of vascular SMCs were also negative for TLR7 and TLR9 (Figure IA and IB in the online-only Data Supplement). Negative controls showed no staining (Figure IC in the online-only Data Supplement). The area with positive staining for both TLRs contained many macrophages, whereas in mice with normal cholesterol these lesions hardly show any of these cells. (Figure ID and IE in the online-only Data Supplement).

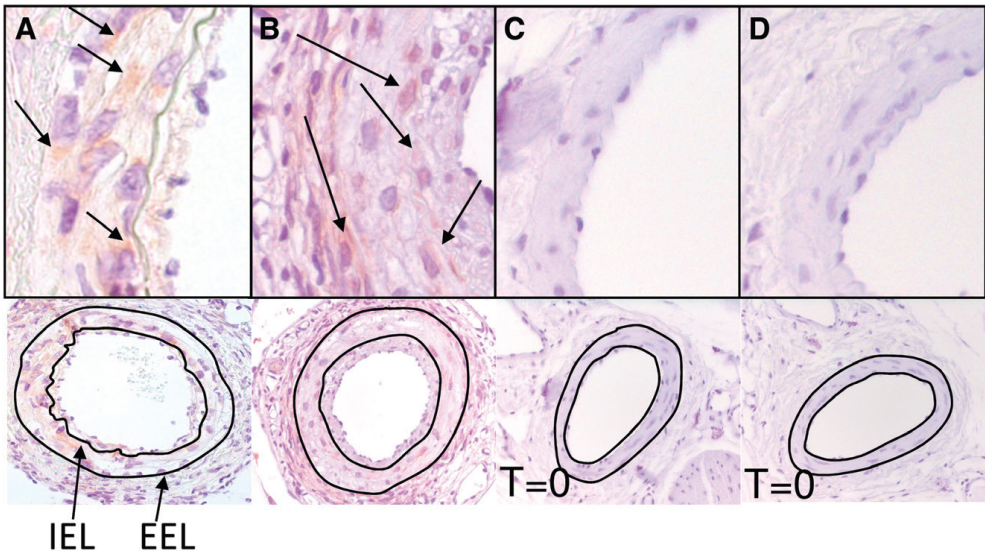

Figure 1. Toll-like receptor (TLR) expression in injured femoral artery lesions of hypercholesterolemic apolipoprotein E*3-Leiden (apoE3*-Leiden) mice. TLR7 expression (A) and TLR9 expression on femoral arteries with neoinitma 14 days after cuff placement (B). Noncuffed femoral arteries stained for TLR7 (C) and TLR9 (D). EEL indicates external elastic lamina; IEL, internal elastic lamina.

Inhibition of TLR7- and TLR9-Mediated Immune Responses by Antagonist

Splenocytes were cultured with 0.01 to 10 μg/mL of the dual TLR7/9 antagonist in combination with TLR3, TLR4, TLR7, or TLR9 agonist. The antagonist showed a dose-dependent reduced production of TNF, IL-6, and IFN-γ–induced protein 10 on either TLR7 or TLR9 activation. Activation of TLR4, the most robust signaling TLR, was not affected. Also cytokine production via activation of intracellular TLR3, which recognizes double-stranded RNA, was not affected by the antagonist (Figure IIA–IID in the online-only Data Supplement). Culturing of splenocytes with the antagonist alone did not induce cytokine production (not shown). Administration of either TLR7 or TLR9 agonists alone to mice resulted in elevated inflammation indicated by increased levels of serum IL-12. Mice administered with antagonist before TLR7 or TLR9 agonist administration displayed lower levels of serum IL-12. TLR7/9 antagonist alone did not induce IL-12 expression, suggesting it does not induce immune responses. At the dose used, antagonist showed ≈64% and 85% inhibition of TLR9 and TLR7 agonist-induced IL-12 in mice, respectively. (Figure III in the online-only Data Supplement). Control oligo showed no inhibition of either TLR7- or TLR9-mediated immune response in mice (Figure 2).

TLR7/9 Antagonist Reduced Neointima Formation and Accelerated Atherosclerosis

After detecting TLR7 and TLR9 presence in remodeled arteries, we focused on vascular remodeling. By in vivo administration of the antagonist, the causal involvement of TLR7/9 activation in intimal hyperplasia and accelerated atherosclerosis was assessed in hypercholesterolemic apoE*3-Leiden mice that underwent femoral arterial cuff placement, a widely applied model for restenosis. These mice were fed a Wes

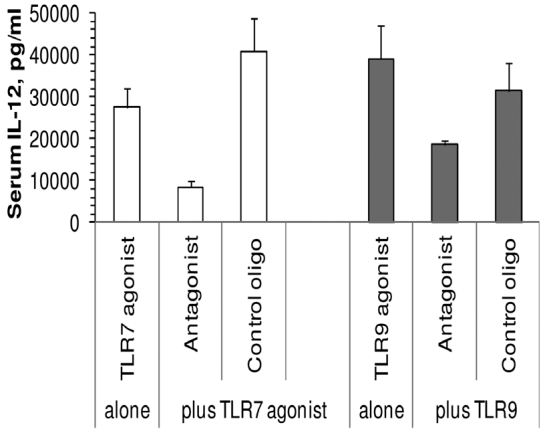

Figure 2. Antagonist or control oligo was injected at 5 mg/kg, s.c. in the left flank of 6- to 8-week-old female C57BL/6 mice (n=2/group). RNA-based toll-like receptor 7 (TLR7) agonist at 10 mg/kg, s.c. or TLR9 agonist at 0.25 mg/kg, s.c. was injected 48 hours later in the right flank. Two hours post-TLR agonist administration, blood was collected, and serum interleukin-12 (IL-12) level was determined by ELISA. TLR7 or TLR9 agonist alone was used as a positive control. Data shown are representative of at least 2 independent experiments.

tern-type diet, starting 3 weeks before surgery to induce hypercholesterolemia, and are well known to develop intimal lesions attributable to neointima formation and accelerated atherosclerosis. No significant difference in plasma total cholesterol levels was detected before surgery (control 9.3±0.60 mmol/L; TLR7/9 antagonist 9.0±0.46 mmol/L), nor had antagonist-treated mice significant altered cholesterol levels compared with control mice after 14 days at euthanizing (control 8.4±0.4 mmol/L; TLR7/9 antagonist 7.7±0.8 mmol/L). Hematoxylin-phloxine-saffron–stained sections were used to study vessel wall composition and showed a profound neointima formation with foam cell formation, which was clearly reduced in the antagonist-treated group. After quantification, we observed reduction in neointima formation of 66% (n=9 versus n=7; 5838±1158 μm^2 versus 2008±223 μm^2; P=0.0079), a beneficial intima/media ratio (0.473±0.09 μm^2 versus 0.168±0.018 μm^2; P=0.0021), and a reduction in percentage of lumen stenosis of 64% (33.9±6.6% versus 12.5±2.9%; P=0.0021) after administration of antagonist biweekly. No differences in total vessel wall area or media area were found (Figure 3A–3G). In addition, we found a difference in IL-10 serum levels that were significantly higher in the antagonist-treated mice 14 days after cuff placement (0.43 versus 15.46 pg/mL; P=0.0003; Figure IV in the online only Data Supplement). At euthanizing, the antagonisttreated mice had a higher number of circulating Ly6Clow monocytes compared with PBS-treated controls (Figure V in the online-only Data Supplement). In the lesions of the antagonist-treated mice, a reduced number of macrophages (MAC3-positive cells) was observed (Figure 3). This difference may be attributable to reduced infiltration of the vessel wall by the circulating monocytes because the expression of adhesion molecule CD11b was decreased on the cells of the antagonist-treated mice (Figure 3H). Nonspecific oligonucleotide administration not only had no effect on the number of circulating (Ly6Clow) monocytes or CD11b expression compared with PBS treatment, it also did not affect neointima formation (Figure 3I and 3J).

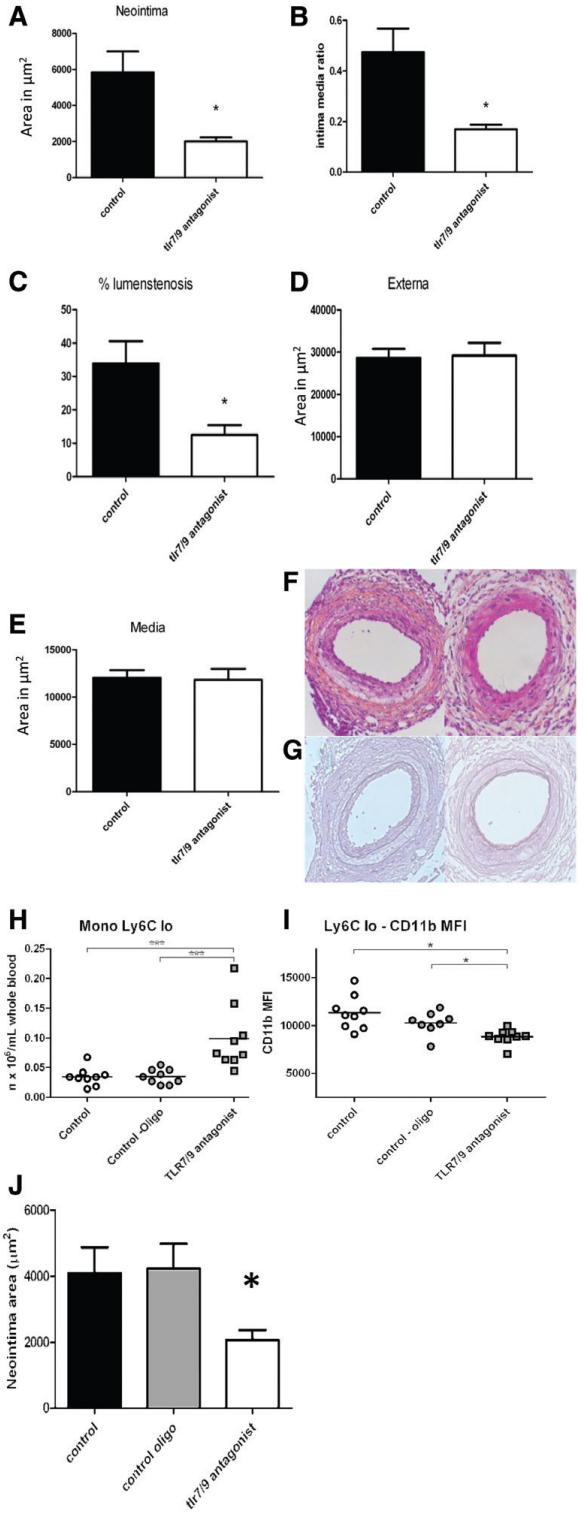

Figure 3. Restenosis with accelerated atherosclerosis was initiated via cuff placement around the femoral artery in hypercholesterolemic apolipoprotein E*3-Leiden (apoE*3-Leiden) mice. Areas of femoral arteries were quantified by using 6 sections per vessel of each mouse. A mean of these 6 sections was used as the outcome of arterial remodeling per mouse. Outcomes of analysis are expressed in µm² (mean±SEM). Mice treated with the antagonist showed a significant reduction in neointima formation compared with controls (A). Antagonist-treated mice also showed a decrease in percentage of lumen stenosis (B) and a beneficial intima/media ratio (C). Neither total vessel wall area nor media area were altered (D and E). Representative hematoxylinphloxine-saffron (HPS; F) and Weigert elastin (G) stained cross sections of control mice and antagonist-treated mice 14 days after cuff placement. Number of circulating Ly6clow monocytes (corrected for total white blood cell count; H). Expression of adhesion molecule CD11b on Ly6clow monocytes (I). Neointima formation of cuffed mice treated with PBS, control oligo, and toll-like receptors 7 and 9 (TLR7/9) antagonist (J). *P<0.05. Statistical analysis was performed by use of a nonparametric Mann-Whitney test, *P<0.05. MFI indicates mean fluorescence intensity.

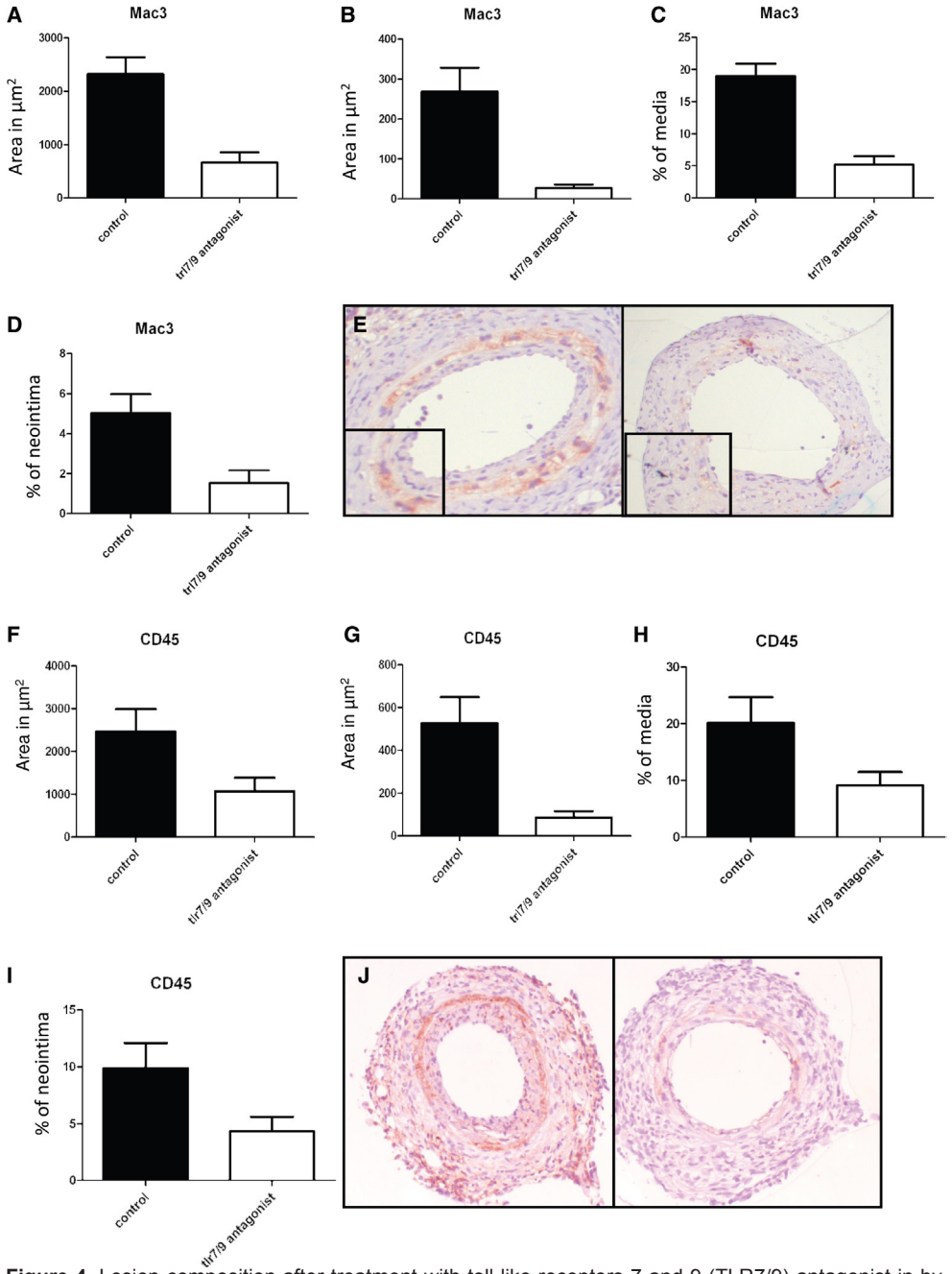

Figure 4. Lesion composition after treatment with toll-like receptors 7 and 9 (TLR7/9) antagonist in hypercholesterolemic apolipoprotein E*3-Leiden (apoE*3-Leiden) mice. Sections were stained for MAC3 and CD45. Positive staining in areas of femoral arteries was quantified by using 6 sequential sections per artery of each mouse. A mean of positive staining of these 6 sections was used as the outcome of positive immunostaining per mouse. Outcomes of analysis are expressed in µm^2 (mean±SEM) and percentage of area of either media or neointima. Macrophage infiltration was significantly reduced in the antagonist-treated group compared with the controls in both neointima (A) as well as media (B). Percentage of positive staining for MAC3 was reduced in this group in both media (C) and neointima (D). Resentative

pictures of control mice and antagonist-treated mice (E). Leukocyte infiltration in the antagonist-treated group compared with the controls in media (F) as well as neointima (G). Percentage of positive staining for CD45 in the media (H) and neointima (I). Representative pictures of CD45 stained sections of control mice and antagonist-treated mice (J). Statistical analysis was performed with a nonparametric Mann-Whitney test, *P<0.05.

TLR7/9 Blockade Reduced Macrophage/Foam Cell-Positive Area

As stated above, we observed a significant reduced MAC3-positive area. This was the case in both media (2445±327 μm^2 versus 661±199 μm^2; P=0.002) as well as neointima (268±59 μm^2 versus 26±9 μm^2; P=0.003), indicating less infiltration of macrophages that are importantly involved in the remodeling process. The percentage of positive area was also significantly reduced indicating a reduction of positive cells per μm^2 in both media as well as in the formed neointima. We also checked whether the effects observed in vivo could be related to the accumulation of total leukocytes in the lesions. Therefore, we quantified the area of the vessel segments that was positive of CD45, a pan-leukocyte marker. Vessels of the antagonist-treated mice showed a trend toward a reduced CD45-positive area which was significant in the neointima (Figure 4A–4J).

TLR7/9 Blockade Reduced Cytoplasmic HMGB1

Layers in the vessel wall undergo severe stress on intervention. Together with our finding of a significant decrease in macrophages, we searched for the presence of cytoplasmic or extracellular HMGB1 that is a marker of cell stress and macrophage activation. HMGB1 can be directly upregulated by TLR9 activation and is an important TLR7/9 signaling regulator and an endogenous TLR2/4 ligand. Kalinina et al previously showed that HMGB1 could be detected in atherosclerotic plaques. Furthermore, the authors showed that this was dominant in macrophages, and that in these macrophages there was a marked increase of HMGB1 in the cytoplasm.[25] Therefore, we performed analysis for the presence of cytoplasmic HMGB1 in the arterial wall. Because TLR7/9 was predominately expressed in the tunica media, where most macrophages/foam cells were present, the media area of the vessel segments that was positive for HMGB1 outside the nucleus was quantified. We found a significant decrease in the percentage of positive cytoplasmic HMGB1 in the media area of mice treated with antagonist (12.97±1.03% versus 7.80±1.28%; P=0.011; Figure 5A–5C). This is of special interest, because HMGB1 release is increased on TLR7/9 activation, regulates TLR7/9 signaling, and is known to function as an endogenous ligand for TLR2 and TLR4 (Figure 5A–5C).

TLR7/9 Blockade Reduced Macrophage Proinflammatory Cytokine Production on TLR7/9 Activation

Macrophage activation and foam cell accumulation play a crucial role in lesion formation and accelerated atherosclerosis development after cuff placement. Because we found less macrophages and HMGB1 after blocking TLR7/9, we studied the effects of modulation of the TLR7/9 signaling in cultured bone marrow–derived macrophages. Bone marrow–derived macrophages were cultured for 7 days, and then stimulated with either TLR7 ligand imiquimod, TLR9 ligand C-phosphate-G (CpG)-oligodeoxynucleotide, or a combination of both for 24 hours. Activation was monitored by analysis of TNF-α expression, a key proinflammatory cytokine also known to

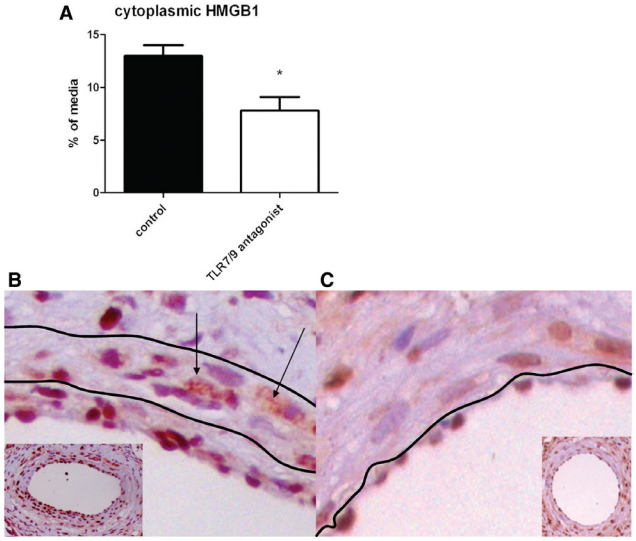

Figure 5. Presence of cytoplasmic highmobility group box 1 (HMGB1) in the injured vessel wall of hypercholesterolemic apolipoprotein E*3-Leiden (apoE3*Leiden) mice 14 days after surgery. Sections were stained for HMGB1. Positive staining in areas of femoral arteries was quantified by using 6 sequential sections per artery of each mouse. A mean of positive staining of these 6 sections was used as the outcome of positive immunostaining per mouse. Outcome of cytoplasmic HMGB1 analysis in percentage (mean±SEM) of area of media (A). Representative pictures of HMGB1 staining in control mice (B) and antagonisttreated mice (C). Statistical analysis was performed with a nonparametric Mann-Whitney test, *P<0.05. TLR7/9 indicates toll-like receptors 7 and 9.

be regulated in vivo after cuff placement.[26] Coadministration of TLR7/9 ligands with the antagonist caused a significant reduction in the production of TNF-α, whereas lipopolysaccharide-induced production of TNF-α was not altered by the antagonist (Figure 6A).

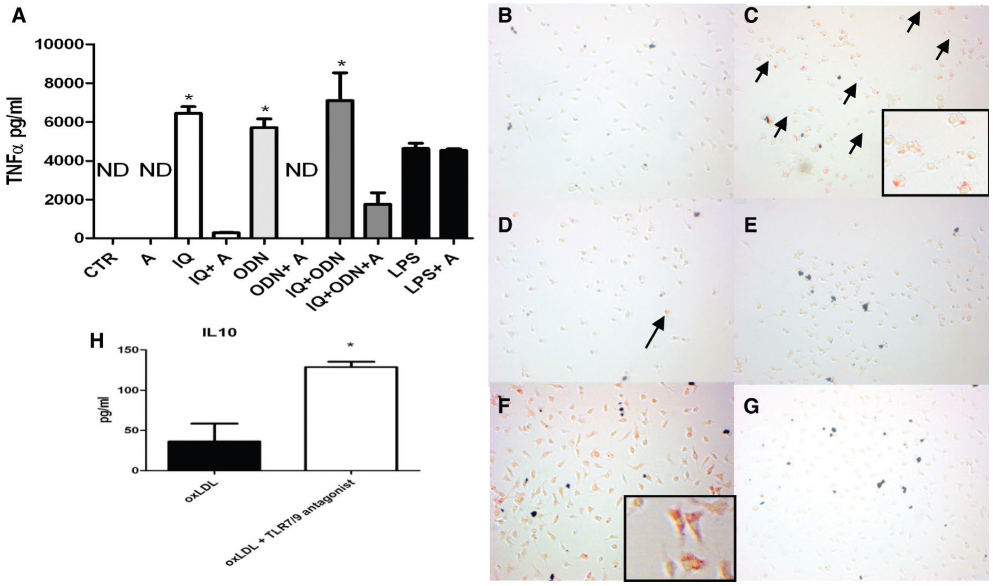

Figure 6. Bone marrow–derived macrophages cultured with imiquimod (IQ) as a ligand for toll-like receptor 7 (TLR7), C-phosphate-G–oligodeoxynucleotide (CpG-ODN) as a ligand for TLR9 or TLR7/9 antagonist for 24 hours. IQ and CpG induced macrophage activation. Use of the TLR7/9 antagonist caused a decrease in tumor necrosis factor-α (TNF-α) production. TLR4- (lipopolysaccharide, [LPS]) induced activation was not altered by the antagonist. A, Foam cell formation was studied on cultured macrophages in the presence of empty medium, native low-density lipoprotein (LDL), IQ, IQ+LDL, and IQ+LDL+antagonist. All wells were screened for positive Oil Red O (ORO) staining, and representative pictures are shown. Macrophages with native LDL showed no lipid uptake after staining with ORO (B). Positive staining in the presence IQ with native LDL (C), IQ+LDL+antagonist (D), and IQ (E). Foam cell formation independent of direct TLR activation was studied on cultured macrophages in the presence of oxidized LDL (oxLDL) or oxLDL+antagonist. All wells were screened for positive ORO staining, and representative pictures are shown. Macrophages with oxLDL showed lipid uptake after staining with ORO (F) but only a few positive spots in the presence of TLR7/9 antagonist (G). Analysis by ELISA showed a significant difference in interleukin-10 (IL-10) levels in the presence of TLR7/9 antagonist (H). Student t test was used for statistical analysis, *P<0.05. CTR indicates control.

TLR7/9 Blockade Reduced Foam Cell Formation by Macrophages

Additionally to the direct effect of proinflammatory cytokine excretion by macrophages, we looked into the effect on lipid accumulation by macrophages because both processes are important in postinterventional remodeling. Because macrophage-induced cytokine production and foam cell formation are major contributors to neointima formation and accelerated atherosclerosis, we studied whether TLR7 activation in combination with native LDL could induce lipid uptake by macrophages as was shown previously for TLR9. Reduced TLR9 activation was previously described to be important in foam cell formation via oxidation of native LDL-cholesterol that normally is not capable of causing foam cell formation.[27] Furthermore, we were interested in whether our antagonist could block this process efficiently like it did on inflammation with only the agonists. Presence of native LDL with TLR7 stimulation alone caused lipid accumulation shown by positive Oil Red O staining in the macrophages whereas native LDL-cholesterol alone showed no staining at all (Figure 6A and 6B). The use of antagonist showed a clear reduction in lipid uptake, and thus foam cell formation indicated less intracellular Oil Red O staining in the fixed macrophages (Figure 6B–6E). TLR9 activation and blockade in the presence of LDL gave the same results, and was described previously[27,28] (data not shown). Foam cells, formed by oxidized LDL (oxLDL) uptake of macrophages, die of releasing lipids, intracellular molecules, and necrotic debris which can further activate the
remaining macrophages via endosomal receptors like TLR7/TLR9.[29] Therefore, we cultured macrophages in the presence of oxLDL cholesterol (Figure 6F) to check whether the antagonist also could influence this lipid accumulation if we combined oxLDL administration with the antagonist. Oil Red O staining was found in the oxLDL-treated macrophages, whereas in combination with the antagonist showed only a few slightly positive cells (Figure 6F and 6G). To see whether this effect was dependent on influx or efflux of lipids, we analyzed expression of scavenger receptor CD36 and IL-10 production. CD36 scavenger receptor expression was not different (positive CD36 macrophages; control 41.48% versus antagonist 41.32%; Figure V in the online-only Data Supplement), however we noticed significant change in IL-10 levels (Figure 6G) indicating effects on lipid efflux whereas IL-10 enhances lipid efflux via the peroxisome proliferator-activated receptor-γ-liver X receptor- ATP-binding cassette subfamily A member 1/ATP-binding cassette subfamily G member 1 pathway.[30]

Discussion

The present study describes the role of a novel TLR7/9 dual antagonist in restenosis and accelerated atherosclerosis in mice. Individual presence of both TLR7 and TLR9 was noticed in femoral arteries of hypercholesterolemic apoE*3-Leiden mice with neointimal lesions and accelerated atherosclerosis after 14 days. These have to be infiltrating cells (eg, macrophages), whereas normal arteries or arterial lesion from normal mice that consist dominantly of vascular SMC stained negative for both TLRs and macrophages. In vivo administration of antagonist showed a significant reduction in neointima formation with a beneficial intima/media ratio in hypercholesterolemic apoE*3-Leiden mice. Moreover, blockade of TLR7/9 signaling led to a reduction in CD45- and MAC3-positive cells in both media as well as in the neointimal lesions, and we notice a decrease in cytoplasmic HMGB1 indicating a decrease in cellular stress and a difference in serum IL-10. In vitro, macrophages showed a significant increase in TNF-α production on TLR7 or TLR9 activation that was reduced after receiving TLR7/9 dual antagonist. Administration with TLR7 ligand imiquimod or TLR9 agonist CpG caused lipid accumulation in macrophages that could be sufficiently blocked by the antagonist. Moreover, oxLDL-induced foam cell formation was inhibited by antagonist, possibly via upregulation of IL-10.

Previously, we and others described involvement of TLR2 and TLR4 in postinterventional neointima formation.[3,6,7] Recently, a protective role for intracellular receptor TLR3, important in recognition of double-stranded RNA, was found in vascular remodeling.[31] Neointima formation attributable to postinterventional remodeling is strongly mediated by local activation and physiological changes, such as increased wall stress, cell damage, and inflammation. In the present study, we were able to notice the presence of TLR7 and TLR9 in the postinterventional remodeled arteries whereas noncuffed vessels show no presence of these TLRs at all. This can probably be related to leukocytes that express these TLRs and infiltrate the vessel wall as a result of the damage of the intervention such as macrophages, and start to clear apoptotic cells and infiltrated lipids. The level of TLR expression may vary among different vessel specimens and may be influenced by these changes.[12] Other studies in addition to the present showed TLR7 expression in atheroma of carotids[13] and TLR9 presence in human atherosclerotic plaques[14] that may be activated via unmethylated CpG motifs from bacteria.[32] Furthermore, DNA from 17 different bacterial genera that can activate TLR9 was found in atherosclerotic carotids,[15] together indicating a possibly important contribution of these pattern recognition receptors to vascular remodeling.

Blocking TLR7/9 signaling by antagonist strongly inhibited neointima formation thereby reducing the percentage of lumen stenosis. Neointima formation is strongly mediated by SMC proliferation/migration and macrophage activation and lipid uptake. Because TLR7/9 presence could not be detected in undamaged arteries, it is unlikely that there is a direct activation of SMC. However, indirect activation of SMC is still possible via cytokines produced by leukocytes which express these TLRs. Our results may be explained, at least in part, by the difference in IL-10 production. On the other hand, TLR7 and TLR9 stimulation by their ligands causes a strong increase in the upregulation of TNF-α, which is important in postinterventional vascular remodeling, indicating a direct influence of TLR7/9 activation on inflammation. This

response was nicely blocked by the antagonist in macrophages. Furthermore, we observed lower levels of HMGB1 in the cytoplasm after cuff placement in the antagonist-treated mice, thereby reducing its effect via direct activation of TLR2/4 and activation of intracellular TLRs via its binding to their nucleic acid ligands.[21,33] Moreover, there were significantly fewer numbers of macrophages/foam cells present in media as well as neointima.

Activation of TLR7/9 leads to nuclear factor-kappaB–mediated upregulation of proinflammatory cytokines. Furthermore, it is known that TLR9 activation causes release of nuclear HMGB1 that may become available in the cytoplasm or even outside the cell, where it is known to act as TLR2 and TLR4 ligand and was seen in macrophages in atherosclerotic plaques.[22,25,33,34] Not only can this release be initiated on cell stress but also on activated macrophages that are capable of releasing HMGB1.[34,35] Previously, we were able to detect HMGB1 in remodeled vein grafts in and outside the nucleus.[4] On cuff placement, we noticed the presence of HMGB1 in the cytoplasm as well. Others previously showed that CpG-oligodeoxynucleotide stimulates macrophages to secrete HMGB1, and extracellular HMGB1 is known to accelerate the delivery of CpG-oligodeoxynucleotides to its receptor, leading to a TLR9-dependent enhancement of IL-6, IL-12, and TNF-α.[22] Interestingly, HMGB1 is also known as a regulator of TLR7/9 signaling itself because the absence of HMGBs also severely impairs the activation of TLR3, TLR7, and TLR9 by their cognate nucleic acids.[21] Therefore, these intracellular TLRs are thought to play a very important role in autoimmune and other inflammatory diseases.[20,21] Our data confirm causal involvement of TLR7 and TLR9 in vascularrelated diseases, and development of a novel TLR7/9 dual antagonist may have important implications for understanding and treatment of exacerbation periods of other inflammatory diseases such as rheumatoid arthritis and after vascular interventions that cause direct vessel damage.

Blocking TLR7/9 signaling leads to a reduction in inflammation and reduced lipid accumulation. The role for TLR7/9 may therefore indicate regulation of cell stress and thereby providing activation of macrophages to start scavenging lipids, dying cells, and attracting more leukocytes to the inflammatory hazard. Our results confirm macrophage activation via TLR7/9 ligands and show a decrease of the presence of macrophages in the vessel wall after cuff placement in the TLR7/9 antagonist-treated mice.

Several studies have demonstrated the effect of intracellular TLR activation on lipid uptake.[27,28,36,37] Both TLR7 and TLR9 agonists cause upregulation of adipocyte differentiationrelated protein that is involved in lipid droplet formation in macrophages.[38] TLR9 was previously described to be involved in foam cell formation via upregulation of nicotinamide adenine dinucleotide phosphate oxidase 1, lectin-type oxLDL receptor 1, and perilipin 3.[27,28] This foam cell formation was nuclear factor-kappaB– and IFN regulatory factor 7–dependent, and can be countered via liver X receptor activation.[37] Both nuclear factor-kappaB and IFN regulatory factor 7 are also important mediators of TLR7 signaling, and additionally we show that TLR7 stimulation in the presence of LDL leads to lipid uptake in macrophages. Our data show that blocking of TLR7 receptor results in no lipid uptake in macrophages that receive only LDL. Interestingly, the antagonist was capable of decreasing lipid accumulation of oxLDL in macrophages probably via IL-10. This might be attributable to altered efflux of lipids rather than decreased influx because CD36 expression is not altered whereas

IL-10, like in vivo, is upregulated. Macrophage IL-10 is known to enhance the efflux of cholesterol.[30] Different mechanisms, directly related to TLR signaling, can be involved in changing IL-10 levels. Martin et al.[39] showed that glycogen synthase kinase 3 can differentially regulate TLR-mediated cytokine production. In the normal TLR activation situation, there is little phosphatidylinositol 3-kinase stimulation, and glycogen synthase kinase 3 primarily remains constitutively active promoting the expression of IL-12. Alternative situations, with different pathogenic stimuli or blocking antagonists (small molecule inhibitors, RNA inhibitors), can lead to TLR-dependent activation of phosphatidylinositol 3-kinase and thereby inhibition of glycogen synthase kinase 3 that causes a decrease in IL-12 production and an increase in IL-10 production. Woodgett and Ohashi[40] have provided a nice overview about this glycogen synthase kinase 3 in TLR signaling. Alternatively, it was previously described that TLR4 activation can cause an increase of HMGB1 in macrophages, and that this HMGB1 is capable of reducing IL-10 levels.[41] OxLDL triggers inflammatory signaling through a heterodimer of TLR 4 and TLR6. Assembly of this newly identified heterodimer is regulated by signals from the scavenger receptor CD36.[42] Foam cells die of releasing lipids, intracellular molecules, and necrotic debris which can further activate the remaining macrophages via endosomal receptors like TLR7/TLR9.[29] Although HMGB1 can also be upregulated via TLR9 activation and it further enhances TLR7/9 activation, this might be a mechanism that causes the differences seen in IL-10 levels. Previously, it was already shown on regulatory T cells that additional TLR9 activation could inhibit IL-10 synthesis.[43] Further studies are needed to fully elucidate the mechanisms causing differences in IL-10 levels in relation to TLR signaling and blockade.

In summary, we observed upregulation of TLR7/9 expression during arterial restenosis and reduced macrophage activation and foam cell formation after TLR7/9 blockade, which was accompanied with increase in IL-10 production. Additional blocking of TLR7/9 leads to a reduction in neointima formation, increased IL-10 production, reduced macrophage presence in the lesions as well as less HMGB1 release, indicating the important role of TLR7 and TLR9 in postinterventional remodeling via reducing inflammation as well as lipid accumulation, thereby making it an interesting therapeutic target to reduce restenosis and accelerated atherosclerosis after vascular intervention.

References

1. Pires NM, Jukema JW, Daemen MJ, Quax PH. Drug-eluting stents studies in mice: do we need atherosclerosis to study restenosis? Vascul Pharmacol. 2006;44:257–264.
2. Lardenoye JH, Delsing DJ, de Vries MR, Deckers MM, Princen HM, Havekes LM, van Hinsbergh VW, van Bockel JH, Quax PH. Accelerated atherosclerosis by placement of a perivascular cuff and a cholesterol-rich diet in ApoE*3Leiden transgenic mice. Circ Res. 2000;87:248–253.
3. Hollestelle SC, De Vries MR, Van Keulen JK, Schoneveld AH, Vink A, Strijder CF, Van Middelaar BJ, Pasterkamp G, Quax PH, De Kleijn DP. Toll-like receptor 4 is involved in outward arterial remodeling. Circulation. 2004;109:393–398.
4. Karper JC, de Vries MR, van den Brand BT, Hoefer IE, Fischer JW, Jukema JW, Niessen HW, Quax PH. Toll-like receptor 4 is involved in human and mouse vein graft remodeling, and local gene silencing reduces vein graft disease in hypercholesterolemic APOE*3Leiden mice. Arterioscler Thromb Vasc Biol. 2011;31:1033–1040.
5. Michelsen KS, Wong MH, Shah PK, Zhang W, Yano J, Doherty TM, Akira S, Rajavashisth TB, Arditi M. Lack of Toll-like receptor 4 or myeloid differentiation factor 88 reduces atherosclerosis and alters plaque phenotype in mice deficient in apolipoprotein E. Proc Natl Acad Sci USA. 2004;101:10679–10684.
6. Vink A, Schoneveld AH, van der Meer JJ, van Middelaar BJ, Sluijter JP, Smeets MB, Quax PH, Lim SK, Borst C, Pasterkamp G, de Kleijn DP. In vivo evidence for a role of toll-like receptor 4 in the development of intimal lesions. Circulation. 2002;106:1985–1990.
7. Schoneveld AH, Oude Nijhuis MM, van Middelaar B, Laman JD, de Kleijn DP, Pasterkamp G. Toll-like receptor 2 stimulation induces intimal hyperplasia and atherosclerotic lesion development. Cardiovasc Res. 2005;66:162–169.
8. Arslan F, Smeets MB, Riem Vis PW, Karper JC, Quax PH, Bongartz LG, Peters JH, Hoefer IE, Doevendans PA, Pasterkamp G, de Kleijn DP. Lack of fibronectin-EDA promotes survival and prevents adverse remodeling and heart function deterioration after myocardial infarction. Circ Res.2011;108:582–592.
9. Hochleitner BW, Hochleitner EO, Obrist P, Eberl T, Amberger A, Xu Q, Margreiter R, Wick G. Fluid shear stress induces heat shock protein 60 expression in endothelial cells in vitro and in vivo. Arterioscler Thromb Vasc Biol. 2000;20:617–623.
10. Li W, Sama AE, Wang H. Role of HMGB1 in cardiovascular diseases. Curr Opin Pharmacol. 2006;6:130–135.
11. Midwood K, Sacre S, Piccinini AM, Inglis J, Trebaul A, Chan E, Drexler S, Sofat N, Kashiwagi M, Orend G, Brennan F, Foxwell B. Tenascin-C is an endogenous activator of Toll-like receptor 4 that is essential for maintaining inflammation in arthritic joint disease. Nat Med. 2009;15:774–780.
12. Pryshchep O, Ma-Krupa W, Younge BR, Goronzy JJ, Weyand CM. Vessel-specific Toll-like receptor profiles in human medium and large arteries. Circulation. 2008;118:1276–1284.
13. Edfeldt K, Swedenborg J, Hansson GK, Yan ZQ. Expression of tolllike receptors in human atherosclerotic lesions: a possible pathway for plaque activation. Circulation. 2002;105:1158–1161.
14. Niessner A, Sato K, Chaikof EL, Colmegna I, Goronzy JJ, Weyand CM. Pathogen-sensing plasmacytoid dendritic cells stimulate cytotoxic T-cell function in the atherosclerotic plaque through interferon-alpha. Circulation. 2006;114:2482–2489.
15. Erridge C, Burdess A, Jackson AJ, Murray C, Riggio M, Lappin D, Milligan S, Spickett CM, Webb DJ. Vascular cell responsiveness to Toll-like receptor ligands in carotid atheroma. Eur J Clin Invest. 2008;38:713–720.
16. Boulé MW, Broughton C, Mackay F, Akira S, Marshak-Rothstein A, Rifkin IR. Toll-like receptor 9-dependent and -independent dendritic cell activation by chromatin-immunoglobulin G complexes. J Exp Med. 2004;199:1631–1640.
17. Kawai T, Akira S. The role of pattern-recognition receptors in innate immunity: update on Toll-like receptors. Nat Immunol. 2010;11:373–384.
18. Means TK, Latz E, Hayashi F, Murali MR, Golenbock DT, Luster AD. Human lupus autoantibody-DNA complexes activate DCs through cooperation of CD32 and TLR9. J Clin Invest. 2005;115:407–417.
19. Uccellini MB, Busconi L, Green NM, Busto P, Christensen SR, Shlomchik MJ, Marshak-Rothstein A, Viglianti GA. Autoreactive B cells discriminate CpG-rich and CpG-poor DNA and

this response is modulated by IFN-alpha. J Immunol. 2008;181:5875–5884.
20. Krieg AM, Vollmer J. Toll-like receptors 7, 8, and 9: linking innate immunity to autoimmunity. Immunol Rev. 2007;220:251–269.
21. Yanai H, Ban T, Wang Z, Choi MK, Kawamura T, Negishi H, Nakasato M, Lu Y, Hangai S, Koshiba R, Savitsky D, Ronfani L, Akira S, Bianchi ME, Honda K, Tamura T, Kodama T, Taniguchi T. HMGB proteins function as universal sentinels for nucleic-acid-mediated innate immune responses. Nature. 2009;462:99–103.
22. Ivanov S, Dragoi AM, Wang X, Dallacosta C, Louten J, Musco G, Sitia G, Yap GS, Wan Y, Biron CA, Bianchi ME, Wang H, Chu WM. A novel role for HMGB1 in TLR9-mediated inflammatory responses to CpGDNA. Blood. 2007;110:1970–1981.
23. Wang D, Bhagat L, Yu D, Zhu FG, Tang JX, Kandimalla ER, Agrawal S. Oligodeoxyribonucleotide-based antagonists for toll-like receptors 7 and 9. J Med Chem. 2009;52:551–558.
24. Yu D, Wang D, Zhu FG, Bhagat L, Dai M, Kandimalla ER, Agrawal S. Modifications incorporated in CpG motifs of oligodeoxynucleotides lead to antagonist activity of toll-like receptors 7 and 9. J Med Chem. 2009;52:5108–5114.
25. Kalinina N, Agrotis A, Antropova Y, DiVitto G, Kanellakis P, Kostolias G, Ilyinskaya O, Tararak E, Bobik A. Increased expression of the DNAbinding cytokine HMGB1 in human atherosclerotic lesions: role of activated macrophages and cytokines. Arterioscler Thromb Vasc Biol. 2004;24:2320–2325.
26. Monraats PS, Pires NM, Schepers A, Agema WR, Boesten LS, de Vries MR, Zwinderman AH, de Maat MP, Doevendans PA, de Winter RJ, Tio RA, Waltenberger J, 't Hart LM, Frants RR, Quax PH, van Vlijmen BJ, Havekes LM, van der Laarse A, van der Wall EE, Jukema JW. Tumor necrosis factor-alpha plays an important role in restenosis development. FASEB J. 2005;19:1998–2004.
27. Lee JG, Lim EJ, Park DW, Lee SH, Kim JR, Baek SH. A combination of Lox-1 and Nox1 regulates TLR9-mediated foam cell formation. Cell Signal. 2008;20:2266–2275.
28. Gu JQ, Wang DF, Yan XG, Zhong WL, Zhang J, Fan B, Ikuyama S. A Toll-like receptor 9-mediated pathway stimulates perilipin 3 (TIP47) expression and induces lipid accumulation in macrophages. Am J Physiol Endocrinol Metab. 2010;299:E593–E600.
29. Huang Q, Pope RM. Toll-like receptor signaling: a potential link among rheumatoid arthritis, systemic lupus, and atherosclerosis. J Leukoc Biol. 2010;88:253–262.
30. Han X, Kitamoto S, Wang H, Boisvert WA. Interleukin-10 overexpression in macrophages suppresses atherosclerosis in hyperlipidemic mice. FASEB J. 2010;24:2869–2880.
31. Cole JE, Navin TJ, Cross AJ, Goddard ME, Alexopoulou L, Mitra AT, Davies AH, Flavell RA, Feldmann M, Monaco C. Unexpected protective role for Toll-like receptor 3 in the arterial wall. Proc Natl Acad Sci USA. 2011;108:2372–2377.
32. Chen WH, Kang TJ, Bhattacharjee AK, Cross AS. Intranasal administration of a detoxified endotoxin vaccine protects mice against heterologous Gram-negative bacterial pneumonia. Innate Immun. 2008;14:269–278.
33. Park JS, Svetkauskaite D, He Q, Kim JY, Strassheim D, Ishizaka A, Abraham E. Involvement of toll-like receptors 2 and 4 in cellular activation by high mobility group box 1 protein. J Biol Chem. 2004;279:7370–7377.
34. Lotze MT, Tracey KJ. High-mobility group box 1 protein (HMGB1): nuclear weapon in the immune arsenal. Nat Rev Immunol. 2005;5:331–342.
35. Wang H, Bloom O, Zhang M, Vishnubhakat JM, Ombrellino M, Che J, Frazier A, Yang H, Ivanova S, Borovikova L, Manogue KR, Faist E, Abraham E, Andersson J, Andersson U, Molina PE, Abumrad NN, Sama A, Tracey KJ. HMG-1 as a late mediator of endotoxin lethality in mice. Science. 1999;285:248–251.
36. Chen S, Sorrentino R, Shimada K, Bulut Y, Doherty TM, Crother TR, Arditi M. Chlamydia pneumoniae-induced foam cell formation requires MyD88-dependent and -independent signaling and is reciprocally modulated by liver X receptor activation. J Immunol. 2008;181:7186–7193.
37. Sorrentino R, Morello S, Chen S, Bonavita E, Pinto A. The activation of liver X receptors inhibits toll-like receptor-9-induced foam cell formation. J Cell Physiol. 2010;223:158–167.
38. Feingold KR, Kazemi MR, Magra AL, McDonald CM, Chui LG, Shigenaga JK, Patzek SM, Chan ZW, Londos C, Grunfeld C. ADRP/ADFP and Mal1 expression are increased in macrophages treated with TLR agonists. Atherosclerosis. 2010;209:81–88.
39. Martin M, Rehani K, Jope RS, Michalek SM. Toll-like receptor-mediated cytokine production is differentially regulated by glycogen synthase kinase 3. Nat Immunol. 2005;6:777–784.
40. Woodgett JR, Ohashi PS. GSK3: an in-Toll-erant protein kinase? Nat Immunol. 2005;6:751–

752.
41. El Gazzar M. HMGB1 modulates inflammatory responses in LPSactivated macrophages. Inflamm Res. 2007;56:162–167.
42. Stewart CR, Stuart LM, Wilkinson K, van Gils JM, Deng J, Halle A, Rayner KJ, Boyer L, Zhong R, Frazier WA, Lacy-Hulbert A, El Khoury J, Golenbock DT, Moore KJ. CD36 ligands promote sterile inflammation through assembly of a Toll-like receptor 4 and 6 heterodimer. Nat Immunol. 2010;11:155–161.
43. Urry Z, Xystrakis E, Richards DF, McDonald J, Sattar Z, Cousins DJ, Corrigan CJ, Hickman E, Brown Z, Hawrylowicz CM. Ligation of TLR9 induced on human IL-10-secreting Tregs by 1alpha,25-dihydroxyvitamin D3 abrogates regulatory function. J Clin Invest. 2009;119: 387–398.

Supplements

Material and Methods

Animals

All animal experiments were approved by the animal welfare committee of our institute and are performed according to the regulatory guidelines. Ten week old male hypercholesterolemic APOE*3Leiden mice bred in our laboratory were used as previously described elsewhere.[1] Mice were fed a Western-type diet starting three weeks before surgery that was continued throughout the entire experiment. Mice were allocated randomly to different treatment groups. Cholesterol levels were measured one day before surgery and at sacrifice. All mice received water and food ad libitum.

Murine model for neointima formation

Non-constricted polyethelene cuffs were placed around the femoral arteries as a well-established model for neointima formation and accelerated atherosclerosis.[1] Mice were sacrificed 14 days after cuff placement. All mice received a subcutaneous (s.c) injection with either 200µl sterile water (n=9) or 200µl TLR7/9 antagonist (n=7) (15mg/kg dissolved in sterile water) for sufficient blocking of TLR7/9 continuously without infectious complications. The first injection was administrated directly after cuff placement and injections were repeated 4 times (schedule of two injection per week) until sacrifice of the mice.
Antagonist activity for TLR7 and TLR9 was assessed in six-to-eight-week-old female C57BL/6 mice obtained from Charles River Labs, (Wilmington, MA). Experimental procedures were performed according to the approved protocols and guidelines of the Institutional Animal Care and Use Committee of Idera Pharmaceuticals. Mice (n=2) were injected subcutaneously (s.c.) with 5 mg/kg antagonist. This was followed twenty/four hours later by 0.25 mg/kg TLR9 agonist 2 or 10 mg/kg of an RNA-based TLR7 agonist.[3] Two hours post agonist administration, blood was collected by retro-orbital bleeding.

Morphological Quantification

At sacrifice blood was taken for cholesterol measurement and perfusion/fixation was done at 100mmHg with 4% formaldehyde via the left ventricle. Paraffin-embedded cross-sections were stained with either Weigert's Elastin stain or Hematoxilin-Phloxine-Saphrane (HPS) to visualize overall morphology. Six sections (5 µm thick) equally spaced throughout the cuffed segment were used to quantify intimal lesions, media and total vessel size using image analysis software for morphometric analysis (Qwin, Leica, Germany).

Cell cultures and reagents

Macrophages were derived from bone marrow from tibia and femur and seeded at a density of 250.000 cells/well in 6-wells plates and cultured for 7 days in RPMI GlutaMax (Gibco) supplemented with 100U/ml penicillin/streptavidin, 25% Fetal Calf Serum (FCS) and 20µg/ml M-CSF (Myltec Biotechnologies) as described previously.[4] Cells were cultured in the presence of the TLR7 agonist imiquimod (5µg/ml, Invivo-

gen), the TLR9 agonist ODN-CpG (10μg/ml, Invivogen), oxLDL 50μg/ml or native LDL 50μg/ml (Myltec Biotechnologies) and TLR7/9 antagonist (10μg/ml antagonist, Idera Pharmaceuticals). All analysis was done on triplicate wells each in three independent experiments.
C57BL/6 spleen cells ($1x10^6$ cells/ml) were cultured with 0.01 to 10 μg/ml of a TLR7/9 antagonist in combination with 1 μg/ml of a TLR9 agonist (DNA), 200μg/ml of a TLR7 (sRNA) agonist or 50 μg/ml of a TLR4 agonist (LPS) or 1μg/ml TLR3 agonist (Poly I:C). As controls, spleen cells were cultured with medium alone, TLR9, 7, 4 or 3 agonist alone, or highest dose (10 μg/ml) of the TLR7/9 antagonist alone. After 24 hours, culture supernatants were collected and induction of selected cytokines and chemokines was assessed. All analysis was done on triplicate wells each in three independent experiments.

FACS analysis
Circulating monocytes were stained with anti-mouse CD11b (Biolegend 101224) and Ly6C (Bioconnect MCA2389A488). BMD Macrophages (non-stimulated, antagonist, oxLDL or oxLDL+antagonist, 24h) were stained anti-mouse CD36-PE, clone 72-1, isotype Rat IgG2a (Ebioscience) and analyzed by FACS (BDcalibur).

TLR7/9 antagonist
TLR7 and TLR9 antagonist (5'-TGUCG*TTCT-X-TCTTG*CUGT-5'; wherein, G/U are 2'-O-methyl-ribonucleotides, G* is 7-deaza-dG, and X is glycerol linker) was synthesized at Idera Pharmaceuticals on solid support on an automated DNA/RNA synthesizer with phosphorothioate backbone, purified by HPLC, and analyzed. The purity of full-length antagonist was over 93% with the material balance comprised of oligonucleotides shorter than the full-length product (n-1 and n-2) as determined by anion-exchange HPLC, capillary gel electrophoresis and/or denaturing polyacrylamide gel electrophoresis. Sequence integrity was confirmed by MALDI-TOF mass spectral analysis. Antagonist contained less than 0.2 EU/ml of endotoxin, as determined by the Limulus assay (Bio-Whittaker). A novel control oligo was created with similar chemical modulations in the backbone as in our antagonist since these modifications are crucial to the functional activities of the antagonist. The following sequence was used as a control oligo=: 5'-CACCCAAGACAGCAGAAAG-3'; It is a phosphorothioate oligodeoxynucleotide with 2'-O-methyl-ribonucleotides at each end (nucleotides shown in bold).

Assessment of foam cell formation
Foam cell formation was assessed in macrophages that were either stimulated with native LDL 50μg/ml or oxLDL 50μg/ml (Myltec Biotechnologies). Incubation with native LDL was used to study the effect of TLR7 and TLR9 agonists (IQ, and ODN CpG) on lipid accumulation in macrophages, whereas oxLDL was used under conditions where effects the antagonist are studied. Oil-red-O staining of macrophages was used to identify foam cells. Cells were washed with PBS, fixed in 4%formaldehyde and pretreated with 60% isopropanol followed by staining with 1% Oil-Red-O solution (Sigma Aldrich). Cells were washed with 60% isopropanol followed by three times washing with PBS and examined by light microscopy. Foam cell designation required positive Oil-Red-O staining. Each condition was tested in triplicate.

ELISA assays
ELISA assays were performed with cell free supernatant using commercial available kits following the instructions of the manufacturer for TNFα, IL6, IL-10 (BD Biosciences) and IP-10 (Ebioscience).

Immunohistochemistry
Paraffin-embedded sections (5 µm thick) were stained with antibodies against TLR7 (AbD serotec), TLR9 (AbD serotec), CD45 (BD Biosciences), Mac3 (BD Biosciences), HMGB1 (Abcam, Cambridge, United Kingdom) followed by the appropriate secondary antibody (Donkey anti Rabbit, GE Healthcare) (Goat anti Rat, Jackson labs) and incubated with AB complex (Vector laboratories) and were visualized with Novared (Vector laboratories). Slides were counterstained with haematoxylin.
To confirm the specificity of the IHC staining, parallel sections were incubated with 1% PBS/BSA alone without adding the primary antibody or with Rabbit IgG or Rat IgG controls or staining without 1st antibody or staining without the 2nd antibody. Sections were incubated with the secondary antibody, AB complex and were visualized with Novared. Controls were all negative.

Statistics
For to the animal experiments, values are presented as mean ± standard error of the mean (SEM). Statistical significance was calculated in SPSS for Windows 17.0. Differences between groups were determined using a non-parametric Mann-Whitney test. In vitro assays are presented as mean ± standard error of the mean (SEM) and were statistically analyzed with a students T test.

References

1. Lardenoye JH, Delsing DJ, De Vries MR, Deckers MM, Princen HM, Havekes LM, van Hinsbergh VW, van Bockel JH, Quax PH. Accelerated atherosclerosis by placement of a perivascular cuff and a cholesterol-rich diet in ApoE*3Leiden transgenic mice. Circ Res 2000;87:248-253.
2. Yu D, Wang D, Zhu FG, Bhagat L, Dai M, Kandimalla ER, Agrawal S. Modifications incorporated in CpG motifs of oligodeoxynucleotides lead to antagonist activity of toll-like receptors 7 and 9. J Med Chem 2009;52:5108-5114.
3. Kalinina N, Agrotis A, Antropova Y, DiVitto G, Kanellakis P, Kostolias G, Ilyinskaya O, Tararak E, Bobik A. Increased expression of the DNA-binding cytokine HMGB1 in human atherosclerotic lesions: role of activated macrophages and cytokines. Arterioscler Thromb Vasc Biol 2004;24:2320-2325.
4. Monraats PS, Pires NM, Schepers A, Agema WR, Boesten LS, De Vries MR, Zwinderman AH, de Maat MP, Doevendans PA, de Winter RJ, Tio RA, Waltenberger J, 't Hart LM, Frants RR, Quax PH, van Vlijmen BJ, Havekes LM, van der Laarse A, van der Wall EE, Jukema JW. Tumor necrosis factor-alpha plays an important role in restenosis development. FASEB J 2005;19:1998-2004.

Supplemental figures

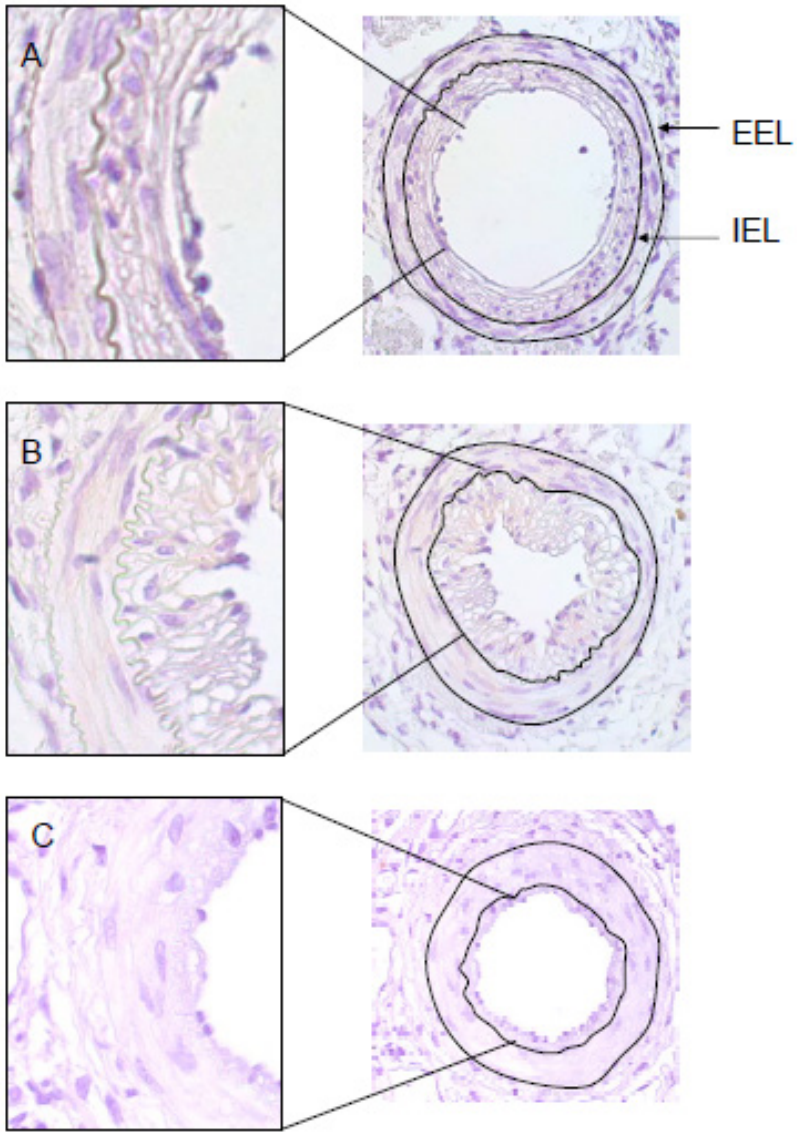

Supplemental figure I: TLR7 staining on arterial lesion of wild type mice (A). TLR9 staining on arterial lesion of wild type mice (B). Example of negative control (C), Macrophage staining in lesions of hypercholesterolemic mice (D) and in wild type mice (E). N= 4 mice per staining; at least 6 sections per mouse were stained for either TLR7 or TLR9. IEL= Internal Elastic Lamina. EEL= External Elastic Lamina

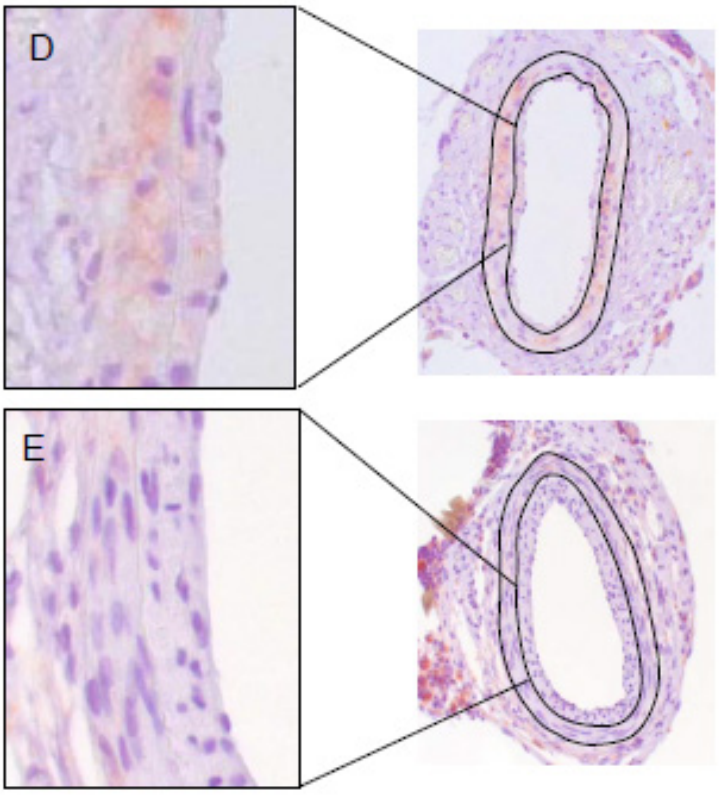

Supplemental figure I: TLR7 staining on arterial lesion of wild type mice (A). TLR9 staining on arterial lesion of wild type mice (B). Example of negative control (C), Macrophage staining in lesions of hypercholesterolemic mice (D) and in wild type mice (E). N= 4 mice per staining; at least 6 sections per mouse were stained for either TLR7 or TLR9. IEL= Internal Elastic Lamina. EEL= External Elastic Lamina

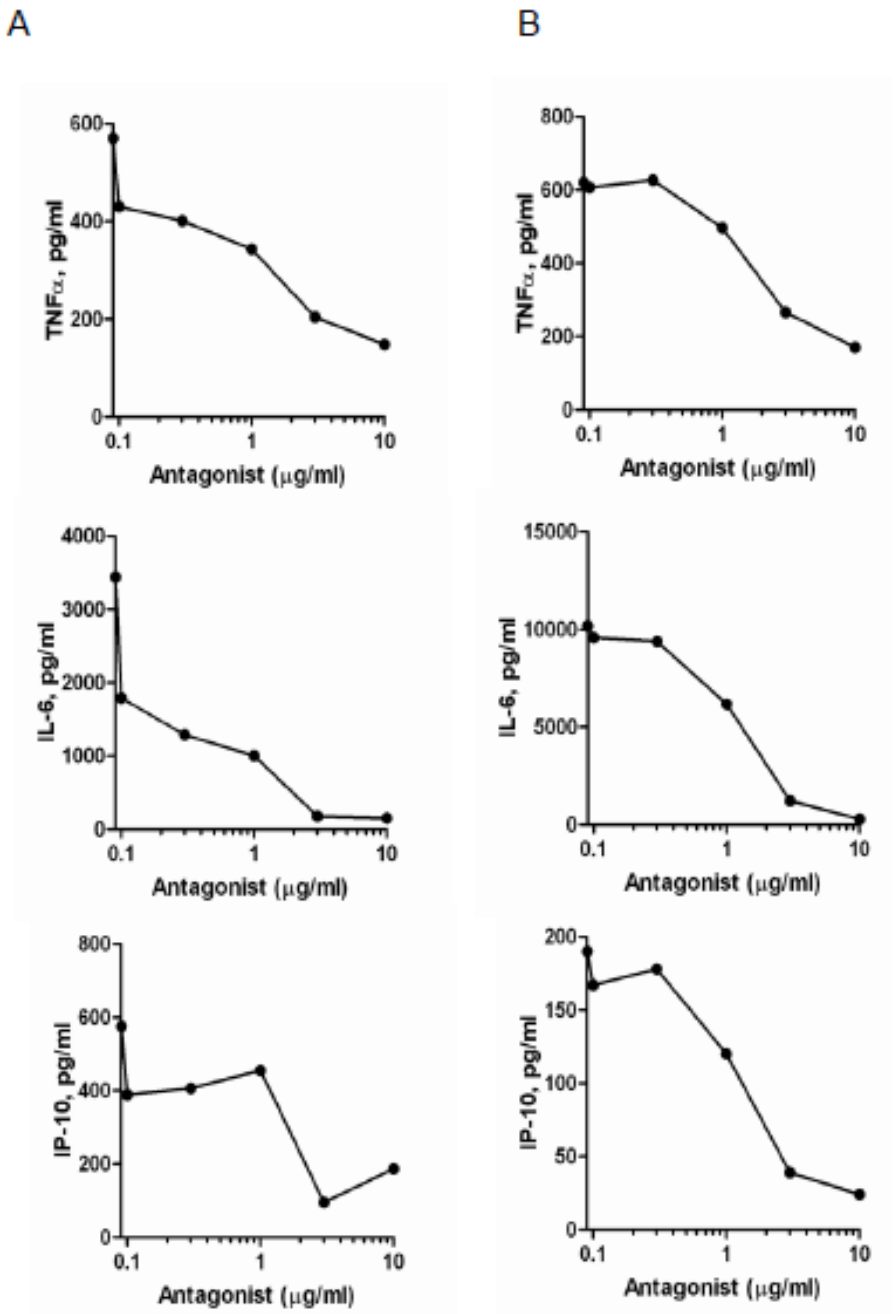

Supplemental figure II: Effect of antagonist on different TLR stimuli. Cytokine production of TNFα, IL6 and IP-10 upon TLR activation in the presence of 0.01 to 10 μg/ml of the TLR7/9 antagonist. TLR7 agonist IQ+ TLR7/9 antagonist (A), TLR9 agonist ODN-CpG + TLR7/9 antagonist (B), TLR3 agonist Polyl:C + TLR7/9 antagonist (C), TLR4 agonist LPS + TLR7/9 antagonist (D). Data shown is 1 representative experiment out of 3 independent experiments.

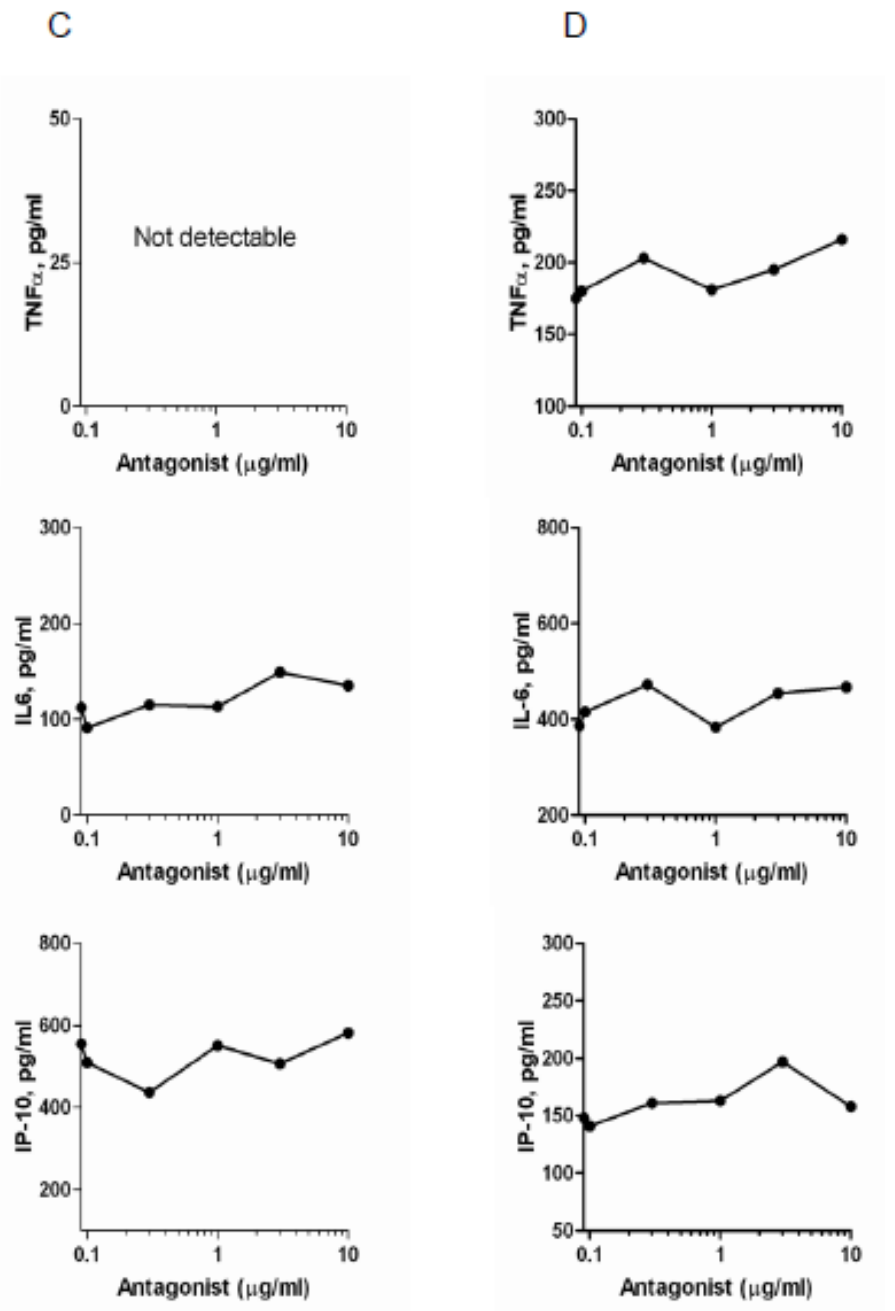

Supplemental figure II: Effect of antagonist on different TLR stimuli. Cytokine production of TNFα, IL6 and IP-10 upon TLR activation in the presence of 0.01 to 10 μg/ml of the TLR7/9 antagonist. TLR7 agonist IQ+ TLR7/9 antagonist (A), TLR9 agonist ODN-CpG + TLR7/9 antagonist (B), TLR3 agonist Polyl:C + TLR7/9 antagonist (C), TLR4 agonist LPS + TLR7/9 antagonist (D). Data shown is 1 representative experiment out of 3 independent experiments.

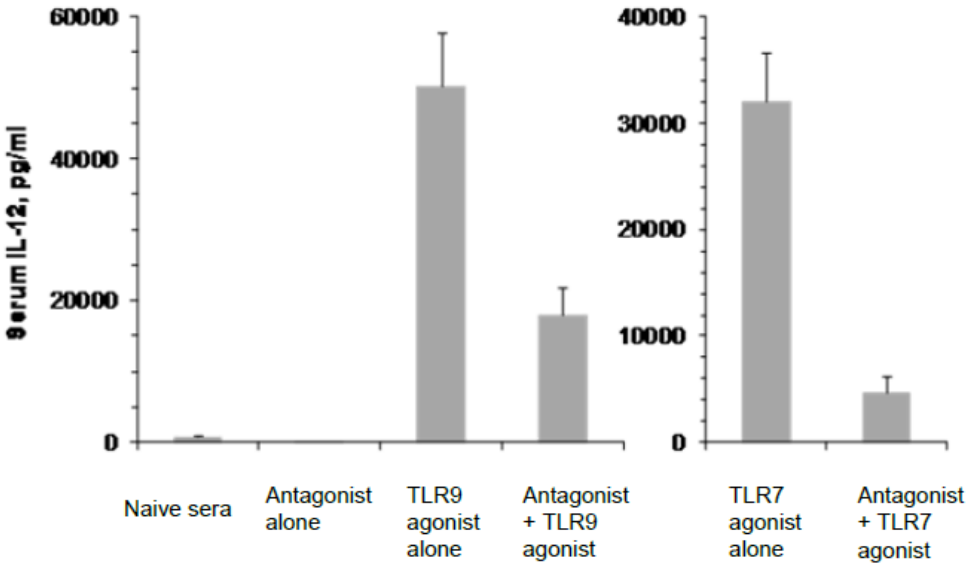

Supplemental figure III: Inhibition of TLR9 and TLR7 agonist induced IL-12 by dual antagonist of TLR7/9 in C57BL/6 mice. Mice (n=2/group) were injected s.c. with 5 mg/kg of antagonist in the left flank and 24 hr later 0.25 mg/kg of TLR9 agonist or 10 mg/kg of TLR7 agonist s.c. in the right flank. Two hours after agonist administration, blood was collected and serum IL-12 levels were measured by ELISA.

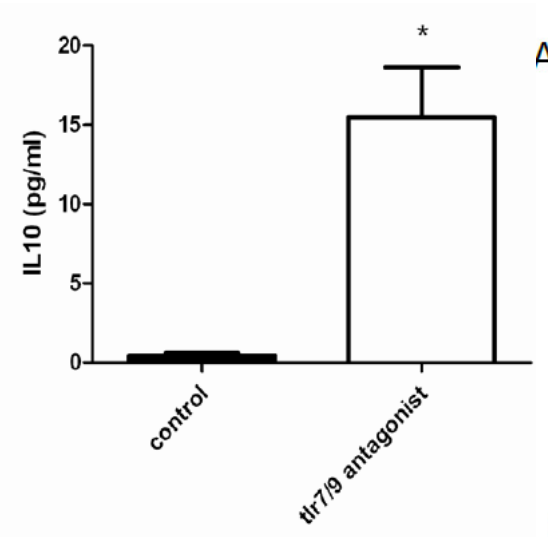

Supplemental figure IV: Plasma IL10 levels in hypercholesterolemic ApoE3Leiden mice treated with or without TLR7/9 antagonist 14days after cuff placement. Statistical analysis was performed by use of a non-parametric Mann-Whitney test, * = P<0.05.

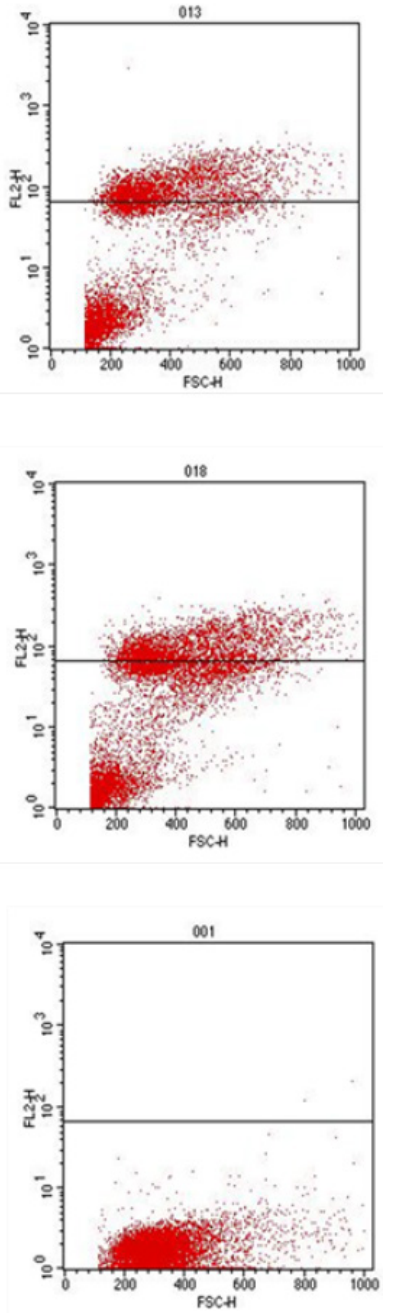

Supplemental figure V: FACS analysis of CD36 expression on oxLDL stimulated macrophages. CD36 expression on macrophages stimulated for 24h with either oxLDL (A) and or with oxLDL in the presence of TLR7/9 antagonist (B) Isotype Control (C).